TECHNICAL INFORMATION SERIES

R62SD7

MASS TRANSFER IN THE HYPERSONIC LOW REYNOLDS NUMBER VISCOUS LAYER

L.GOLDBERG AND S.M.SCALA

SPACE SCIENCES LABORATORY

GENERAL ELECTRIC

MISSILE AND SPACE VEHICLE DEPARTMENT

SPACE SCIENCES LABORATORY

AEROPHYSICS OPERATION

MASS TRANSFER IN THE HYPERSONIC LOW REYNOLDS NUMBER VISCOUS LAYER*

By

Leon Goldberg and
Sinclaire M. Scala

*Presented at the IAS 30th Annual Meeting
New York City, New York, January 22, 1962
Preprint No. 62-80

R62SD07

January 15, 1962

Research performed under the auspices of the United States Air Force, B.S.D. Contract No. AF 04-(647)-617.

MISSILE AND SPACE VEHICLE DEPARTMENT

GENERAL ELECTRIC

CONTENTS

LIST OF FIGURES

ABSTRACT

The low Reynolds number hypersonic flight regime introduces the aerothermochemical interaction of low density hypersonic flow and real surfaces. For the ballistic re-entry of slender bodies or for sustained hypersonic flight at high altitudes, it may prove advantagous to use local mass transfer cooling over certain portions of the surface to reduce the surface temperature where it is expected that oxidation of the surface will otherwise produce excessive shape changes. The effusion of air through a porous surface has been considered in this investigation, and the simultaneous heat and mass transfer processes experienced by hypersonic vehicles flying at high altitudes have been analyzed. Because stagnation region flows represent the severest heating problems, numerical results are presented which are applicable at the forward stagnation point of axi-symmetric hypersonic vehicles.

The governing equations utilized in the present analysis are the equations of change for the flow of a compressible chemically reacting gas. Included were the conservation equations of mass, momentum and energy. The diffusion equations were uncoupled by assuming a Lewis number of unity. Thus, the above system of equations which was treated consists of a coupled set of 4 non-linear partial differential equations of 7th order having split boundary conditions.

For the low Reynolds number regime, all terms of order $1/Re_s$ and larger were retained. The method of separation of variables reduced the governing equations to a set of 5 coupled non-linear ordinary differential equations of order 8 with an "unknown" range of integration. These were then solved numerically utilizing a high speed electronic computer. Note that by utilizing a mass transfer

cooling process, the surface temperature can be maintained at sufficiently low levels so that heterogeneous reactions need not be considered explicitly. The heat transfer, skin friction coefficient and the effectiveness of reducing each by mass transfer were determined over the hypersonic low Reynolds number range of flight speeds from 15,000 ft./sec. to 25,000 ft./sec. and an altitude range from 175,000 ft. to 350,000 ft. The new results were compared with earlier theoretical studies in the continuum regime and in the low Reynolds number regime (without mass transfer), and the differences were interpreted.

LIST OF SYMBOLS

C_f	skin friction coefficient
C_i	mass fraction of species i
C_{p_i}	specific heat at constant pressure of the pure species
$\mathscr{D}_{ij}$	binary diffusion coefficient
f_w	mass transfer parameter (see eq. 57)
h	static enthalpy
h_i	static enthalpy of the i th species, including enthalpy of formation
$\Delta h^o_{f_i}$	enthalpy of formation of the i th species
k	coefficient of thermal conductivity
K_B	nose curvature
$\dot{m}_w$	mass transfer rate ($=\rho_w v_w$)
p	static pressure
Q	heat transfer
$\vec{Q}$	energy flux vector
r	cylindrical radius
R_B	nose radius
T	temperature
u	x-component of velocity
v	y-component of velocity
$\vec{v}$	mass-weighted average velocity of the fluid mixture
$\vec{v}_i$	absolute flow velocity of species i

$\vec{V}_i$ diffusion velocity of species i

V_∞ flight speed

$\dot{w}_i$ net mass rate of production of species i per unit volume by chemical reaction

x, y coordinate system

δ viscous layer thickness

δ_s shock detachment distance

ϵ density ratio across shock ($= \rho_\infty / \rho_s$)

μ ordinary viscosity coefficient

ρ density of fluid mixture

ρ_i partial density of species i

$\mathcal{T}$ viscous stress tensor

Subscripts

s immediately behind shock

w body surface

1, 2 functions of y alone

∞ free stream

Dimensionless Groups

$$C_H = \frac{Q_w}{\rho_\infty V_\infty (H_s - h_w)}$$ Stanton number

$$Le = \frac{\rho \bar{C}_p \mathcal{D}_{ij}}{k}$$ Lewis number

$$Pr = \frac{\bar{C}_p \mu}{k}$$ Prandtl number

$$Re_s = \frac{\rho_\infty V_\infty R_B}{\mu_s}$$ Reynolds number

INTRODUCTION

For slender ballistic re-entry vehicles and hypersonic lifting re-entry vehicles at high altitudes, it is mandatory that adequate information be available for prediction and control of the exchange of mass, momentum and energy between the surface of the vehicle and its environment.

Typical ballistic and lifting re-entry trajectories are shown in Figure 1. Note that Figure 1 is typical for a nominal nose radius equal to one tenth of a foot; for smaller nose radii, all of the low density effects are shifted to lower altitudes.

Descriptive stagnation region velocity profiles are shown to the right of the respective flight regimes. These regimes are discussed below.

As is well known, hypersonic flight at low altitudes is associated with high Reynolds numbers, and a flow field defined by a very thin shock wave followed by an influscid region separated from the body by a thin boundary layer. This is called the ordinary continuum regime, and the whole flow field is known as the shock layer. Conditions directly behind the shock wave are determined using the Rankine-Hugoniot relations and the influscid flow is determined by using one of the available hypersonic shock layer approximations (see, for example Ref. 1); e.g. modified Newtonian, or stream tube, in order to obtain outer boundary conditions for the boundary layer.

For suborbital flight speeds, the radiative heat transfer from the shock layer is very small compared with the aerodynamic heat transfer and hence the dominant energy, momentum and mass transfer processes can all be treated by studying the phenomena within the boundary layer adjacent to the surface. This procedure has yielded many useful solutions to the thermal protection problem, (e.g. Refs. 2-5).

At a somewhat higher altitude (lower Reynolds number) the fluscid effects extend throughout a major portion of the shock layer and the flow may no longer easily be separated into three distinct regions. Convention has now termed this the hypersonic low Reynolds number flow regime which may be divided into two subregimes:

1) Viscous layer - It is still assumed that the classical conservation laws of macroscopic flow are applicable and the shock remains sufficiently thin to be treated as a discontinuity followed by at least a small influscid region.

2) Merged viscous flow - At sufficiently low Reynolds numbers the now thickened shock merges with the fully fluscid flow behind it, and the entire flow field from the free stream to the body surface should be treated as a single problem.

At extreme altitudes, (the free molecule flow regime) it is permissible to neglect collisions between incident and reflected molecules in studying interactions between the vehicle and its environment. However, it is vitally important that the state of the undisturbed gas (Ref. 6), and the surface-particle interactions (Refs. 7-9), be fully taken into account. With decreasing altitude, particles reflected from the surface begin interacting with the incident particles. It becomes necessary to utilize kinetic theory, e.g., the Boltzmann equation (Refs. 10-12) in order to obtain solutions in the near free molecule flow regime.

Between the low Reynolds number and near free molecule flow regimes, a transition regime exists which requires a more rigorous kinetic theory approach, possibly coupled with a macroscopic analysis in which higher order terms are introduced. It should be noted that the uncertainty in the extent of this region is indicated by the lightly shaded area plus the broken line in the velocity profile.

It is seen from Figure 1 that knowledge about the hypersonic low Reynolds number flow regime is important both for slender ballistic entry vehicles and efficient lifting re-entry vehicles. The earliest studies, restricted to order of magnitude analyses, are summarized by Hayes and Probstein (Ref. 1) where the entire hypersonic flight regime is divided into seven subregimes from continuum to free molecule flow, including boundary layer regime, vorticity interaction regime, viscous layer regime, incipient merged layer regime, fully merged layer and transitional layer regimes, first order collision theory regime and free molecule flow regime. This classification scheme has been the basis of most subsequent studies.

In Hoshizaki's study (Ref. 13) of the effect of bluntness-induced vorticity on the boundary layer, it was concluded that the inviscid momentum equations evaluated behind the shock are equivalent to using the vorticity as a boundary condition, and thus, the complete momentum equations incorporate the vorticity boundary conditions. Increases in heat transfer and skin friction were obtained when the vorticity terms were retained in the Navier-Stokes equations, as the Reynolds number was decreased. However, these terms are retained in an appropriate low Reynolds number order of magnitude analysis. In Refs. 14-17, similar results were obtained by appealing to the low Reynolds number nature of the flow without special recourse to vorticity except as a modification of the pressure term.

In Refs. 13-16, the density was assumed constant through the shock layer. Since it can easily be shown that the variation of density through this shock layer is of the same order of magnitude as that across the shock wave, it would appear that the assumption of constant density is not realistic. In a more recent study (Ref. 17), the density variation was taken into account, and it was shown that as the Reynolds

number decreases, the ratio of heat transfer calculated with density variation to the heat transfer calculated with constant density increases. Clearly, then, the variation of density across the viscous layer should be considered in a realistic analysis.

In all of the above studies however, solutions were obtained for the flow of a viscous non-dissociating perfect gas. Hence, these studies ignored the important physicochemical phenomenon of dissociation, which decreases the molecular weight of the gas and alters the relationship between density, temperature and pressure. Also not considered was the alteration in the flow produced by mass transfer from the surface, which will be shown to have a considerable effect upon the structure of the viscous layer and other dependent variables.

In Ref. 14, Probstein and Kemp extended their analysis to the merged viscous layer problem by matching a simplified perfect gas shock structure solution with their constant density perfect gas viscous layer solution. Recently, Levinsky and Yoshihara, Ref. 18, also studied the merged viscous layer but included variable density. Qualitatively, the results appear credible. However, in addition to the remarks made previously about the non-dissociating perfect gas model in the viscous layer solution, its use in the study of hypersonic shock wave structure in air is even more unrealistic, since not only is the gas within a hypersonic shock wave not in chemical equilibrium, it is not even in thermodynamic equilibrium, (Ref. 19) i.e., the relaxation times for the translational degrees of freedom are much shorter than the other degrees of freedom, (e.g. rotational, vibrational). In particular, the available kinetic energy of the molecules is redistributed among many different internal modes of energy storage which absorb energy at different rates, but nevertheless in parallel processes and not in series. It is stressed that the dissociation and ionization

processes which absorb energy and act to reduce the gas temperature, will begin before thermal equilibration is complete.

The present analysis has been carried out in the regime defined in Figure 1 as the hypersonic low Reynolds number viscous layer regime. In this regime, the viscous layer thickness δ is significant compared to the shock detachment distance δ_s, but $\delta/\delta_s < 1$, and the shock wave thickness is sufficiently small so that it can be assumed that the flow is in thermochemical equilibrium behind the shock, before entering the viscous layer.

The governing equations utilized in the analysis are the equations of change for the flow of a compressible chemically reacting gas. Included are the conservation of mass, momentum and energy. In order to simplify the system of equations, the diffusion equations were uncoupled by assuming a Lewis number of unity. The boundary conditions are split; some are specified on the surface and the others behind the shock wave.

To evaluate the remaining transport coefficients, the Prandtl number was assumed to be constant at a value of 0.71 and Sutherland's law was utilized for calculating the viscosity.

Even after expanding the simplified version of the governing equations into the usual body-oriented coordinates, it is necessary to make further simplifying assumptions in order to reduce the system of equations to a more tractable form. It is further assumed that the shock layer thickness δ_s is small compared with a characteristic dimension of the vehicle; in this case the nose radius, R_B. In fact, it has been shown, e.g. Refs. 1, 17, 22,

$$\frac{\delta_s}{R_B} = 0\ (0.1) \qquad (1)$$

in the stagnation region of a hypersonic vehicle. Based on this assumption, the order of magnitude of each term in the expanded governing equations may be calculated. Retaining all terms from order one to those of order $(Re_s)^{-1}$ yields the equations appropriate for a low Reynolds number analysis. Following a procedure similar to that utilized by Probstein and Kemp (Ref. 14), Ho and Probstein (Ref. 17), and Levinsky and Yoshihara (Ref. 18), the four non-linear partial differential equations were reduced to an eighth order set of five non-linear ordinary differential equations with split boundary conditions. The primary additional assumptions introduced were: 1) the shock is concentric with the body, 2) the flow is locally similar and 3) the variables are separable. The following system of equations represents the viscous flow in the forward stagnation region of the hypersonic low Reynolds number viscous layer.

BASIC RELATIONS

The validity of the conservation equations in the continuum regime has been amply demonstrated over the past fifty years. In extending the analysis to lower Reynolds numbers it is assumed that the density is sufficiently large that the same macroscopic governing equations are still applicable. In the absence of external force fields the steady state form of these equations is:

Conservation of Species i

$$\nabla \cdot (\rho_i \vec{v}_i) = \dot{w}_i \tag{2}$$

Conservation of Momentum

$$\rho (\vec{v} \cdot \nabla) \vec{v} = -\nabla p + \nabla \cdot \mathcal{I} \tag{3}$$

Conservation of Energy

$$\rho \vec{v} \cdot \nabla \left(h + \frac{\vec{v} \cdot \vec{v}}{2} \right) = -\nabla \cdot \vec{Q} + \nabla \cdot (\underset{\sim}{\tau} \cdot \vec{v}) \tag{4}$$

Equation of State

$$\rho = \rho \, (h, \, p) \tag{5}$$

Summation over all species yields the global continuity equation

$$\nabla \cdot (\rho \vec{v}) = 0 \tag{6}$$

Implicitly assumed in the above definitions is that the gaseous system is composed of a mixture of chemically reacting perfect gases. Upon neglecting the Dufour effect and the radiative transport of energy, the heat flux vector $\vec{Q}$ is (Ref. 23),

$$\vec{Q} = - k \nabla T + \sum_i \rho_i \vec{V}_i h_i \tag{7}$$

i.e. the sum of the Fourier conduction and the energy transferred by diffusion. From the definition of h, it is seen that

$$\nabla T = \frac{1}{\bar{C}_p} \left[\nabla h - \sum_i h_i \nabla C_i \right] \tag{8}$$

where $\bar{C}_p$ is the frozen specific heat:

$$\bar{C}_p = \sum_i C_i C_{p_i} \tag{9}$$

As a first approximation, it is assumed that the gaseous components with similar thermal and chemical behavior may be treated as a single averaged component so that the sum total can be treated as a binary mixture of "air atoms" and "air molecules". Then, neglecting pressure and thermal diffusion effects, the mass flux with respect to the mass-averaged velocity reduces to the classical Fick's diffusion relation

$$\rho_i \vec{V}_i = - \rho \mathcal{D}_{ij} \nabla C_i \tag{10}$$

Substitution of eqs. (8) and (10) into (7) yields

$$\vec{Q} = -\frac{\mu}{Pr}\left[\nabla h + (Le-1)\sum h_i \nabla C_i\right] \tag{11}$$

Assuming a Lewis number of unity thus yields

$$\vec{Q} = -\frac{\mu}{Pr}\nabla h \tag{12}$$

and the diffusion equations (2) are uncoupled, even for the case of non-equilibrium flow, without resorting to any specific constraint on the chemical source term, i.e. the term $\sum_i \dot{w}_i h_i$ is accounted for implicitly.

With these simplifying assumptions the governing equations appear expanded below for the coordinate system shown in figure 2.

Continuity:

$$\frac{\partial}{\partial x}(\rho u r^j) + \frac{\partial}{\partial y}(\rho v r^j) + K_B r^j \rho v = 0 \tag{13}$$

x-Component of Momentum:

$$\rho\left[u\frac{\partial u}{\partial x} + v\frac{\partial u}{\partial y} + K_B u v\right] = -\frac{\partial p}{\partial x} + \frac{\partial}{\partial y}\left[\mu\frac{\partial u}{\partial y}\right] + K_B\left[(2+j)\,\mu\frac{\partial u}{\partial y} - \frac{\partial}{\partial y}(\mu u)\right] \tag{14}$$

y-Component of Momentum:

$$\rho\left[u\frac{\partial v}{\partial x} + v\frac{\partial v}{\partial y} - K_B u^2\right] = -\frac{\partial p}{\partial y} + \frac{4}{3}\frac{\partial}{\partial y}\left[\mu\frac{\partial v}{\partial y}\right] + \frac{\partial}{\partial x}\left[\mu\frac{\partial u}{\partial y}\right] + j\,\frac{\mu}{r}\frac{\partial u}{\partial y} - \frac{2}{3}\frac{\partial}{\partial y}\left[\mu\left(\frac{\partial u}{\partial x} + j\,\frac{u}{r}\right)\right] \tag{15}$$

Energy:

$$\rho\left[u\frac{\partial}{\partial x}\left(h+\frac{u^2}{2}\right) + v\frac{\partial}{\partial y}\left(h+\frac{u^2}{2}\right)\right] = \frac{\partial}{\partial y}\left(\frac{\mu}{Pr}\frac{\partial h}{\partial y}\right) + (1+j)\,K_B\frac{\mu}{Pr}\frac{\partial h}{\partial y} + \frac{\partial}{\partial y}\left(\mu u\frac{\partial u}{\partial y}\right) + (1+j)\,K_B\,\mu u\frac{\partial u}{\partial y} - K_B\frac{\partial}{\partial y}(\mu u^2) \tag{16}$$

It should be noted that the governing equations presented here are more complete than those given, for example, in Ref. 17, in that all terms ranging from order unity to order $(Re_s)^{-1}$ appear. Although Ho and Probstein state that they have considered all terms ranging from order unity to order $(\epsilon Re_s)^{-1}$, actually one term of order $(\epsilon Re_s)^{-1}$ seems to be missing in the energy equation. However, this introduces no error in their computations since the missing term vanishes identically at the stagnation point.

State:

$$\rho = \rho\ (h,\ p) \tag{17}$$

Viscosity Law:

$$\mu = \mu\ (h, p) \tag{18}$$

At this point then, there are six unknowns u, v, h, p, ρ and μ which may be determined by solving the six equations (13) through (18) simultaneously.

BOUNDARY CONDITIONS

The location of the edge of the viscous layer within the shock layer, and the magnitude of the physical variables at the outer edge of the viscous layer are not known "a priori". Therefore, for convenience, it was decided to integrate the governing equations from the wall to the shock wave, where the physical variables can be calculated.

It was assumed that the shock in the stagnation region is a surface of discontinuity concentric with the body. It was further assumed that thermochemical equilibrium is achieved behind the shock. Use of the Rankine-Hugoniot relations yield the outer boundary conditions behind the shock wave:

$$u\ (x,\ \delta_s) = K_B x V_\infty \tag{19}$$

$$v\left(x, \delta_s\right) = \left(1 - \frac{1}{2} K_B{}^2 x^2\right) \epsilon \, V_\infty \tag{20}$$

$$p\left(x, \delta_s\right) = \left(1 - K_B{}^2 x^2\right)(1-\epsilon) \, \rho_\infty V_\infty^2 \tag{21}$$

$$h\left(x, \delta_s\right) = \left(1-K_B{}^2 x^2\right)(1-\epsilon^2) \, \frac{V_\infty^2}{2} \tag{22}$$

where

$$\epsilon = \frac{\rho_\infty}{\rho_s} \tag{23}$$

It was also assumed that there is no slip or temperature jump at the wall and hence the boundary conditions at the wall are:

$$u(x,0) = u_w = 0 \tag{24}$$

$$v(x,0) = v_w \tag{25}$$

$$h(x,0) = h_w \tag{26}$$

Note that the number of boundary conditions, namely seven, equals the order of the mathematical system.

Although the magnitude of the physical variables can be calculated behind the shock, the distance from the wall to the shock is not known. However, one may introduce a constraint on the family of solutions which is based on the conservation of mass and takes the form:

$$\rho_\infty V_\infty r_s^{1+j} + \rho_w v_w r_w^{1+j} = \int_0^{\delta_s} \rho u (2r)^j \, dy \tag{27}$$

This equation serves to delimit δ_s.

SEPARATION OF VARIABLES

The governing partial differential equations may be solved by means of the technique known as separation of the variables, which has previously proven useful in treating the low Reynolds number viscous layer, (Ref. 14). In the manner utilized by Probstein and Kemp, the following separable forms of the dependent variables were assumed which were suggested by the boundary conditions at the shock wave.

$$u = K_B \, x \, u_1(y) \tag{28}$$

$$v = \left(1 - \frac{1}{2} K_B^{\,2} x^2\right) v_1(y) \tag{29}$$

$$h = \left(1 - K_B^{\,2} x^2\right) h_1(y) \tag{30}$$

$$\rho = \left(1 - \frac{1}{\gamma} K_B^{\,2} x^2\right) \rho_1(y) \tag{31}$$

$$p = \left(1 - K_B^{\,2} x^2\right) p_1(y) - K_B^{\,2} x^2 p_2(y) \tag{32}$$

$$\mu = \left(1 - \frac{\gamma - 1}{2\gamma} K_B^{\,2} x^2\right) \mu_1(y) \tag{33}$$

$$r = x\left(1 + K_B y\right) \tag{34}$$

where the terms with subscripts 1 or 2 are functions of y alone. For convenience, the following non-dimensional forms are introduced:

$$\bar{u} = \frac{u_1}{V_\infty} \;,\; \bar{v} = \frac{v_1}{\epsilon V_\infty} \;,\; \bar{h} = \frac{h_1}{V_\infty^{\,2}/2}$$

$$\bar{\rho} = \epsilon \frac{\rho_1}{\rho_\infty} \;,\; \overline{p_1} = \frac{p_1}{\rho_\infty V_\infty^{\,2}} \;,\; \overline{p_2} = \frac{p_2}{\rho_\infty V_\infty^{\,2}} \tag{35}$$

$$\bar{\mu} = \frac{\mu_1}{\mu_s \, Re_s} \;,\; \bar{y} = K_B y$$

where the subscripts ∞ and s refer respectively to the free stream conditions and to the state immediately behind the shock. Note that the Reynolds number is defined by:

$$Re_s = \frac{\rho_\infty V_\infty}{K_B \mu_s} \tag{36}$$

With the above simplifications the low Reynolds number viscous layer equations reduce to:

$$(\bar{\rho}\,\bar{v})' + (1+j)\frac{\bar{\rho}}{\epsilon}(\bar{u}+\epsilon\,\bar{v}) = 0 \tag{37}$$

$$\frac{\bar{\rho}}{\epsilon}\left[\bar{u}\,(\bar{u}+\epsilon\,\bar{v}) + \epsilon\,\bar{v}\,\bar{u}'\right] = 2(\bar{p}_1 + \bar{p}_2) + (\bar{\mu}\,\bar{u}')' + (2+j)\,\bar{\mu}\bar{u}' - (\bar{\mu}\bar{u})' \tag{38}$$

$$\bar{\rho}\,\bar{v}\,(\epsilon\,\bar{v})' = -\bar{p}_1' + \left[\frac{4}{3}\,\bar{\mu}\,(\epsilon\,\bar{v})'\right]' + (1+j)\left[\bar{\mu}\,\bar{u}' - \left(\frac{2}{3}\,\bar{\mu}\,\bar{u}\right)'\right] \tag{39}$$

$$\frac{\bar{\rho}\,\bar{u}}{\epsilon}(\bar{u}+\epsilon\,\bar{v}) + \bar{p}_2' = 0 \tag{40}$$

$$Pr\;\bar{\rho}\,\bar{v}\,\bar{h}' = \left(\bar{\mu}\,\bar{h}'\right)' + (1+j)\,\bar{\mu}\,\bar{h}' \tag{41}$$

$$\bar{\rho} = \bar{\rho}\,(\bar{h},\ \bar{p}) \tag{42}$$

$$\bar{\mu} = \bar{\mu}\,(\bar{h},\ \bar{p}) \tag{43}$$

where the primes denote derivatives with respect to $\bar{y}$. It is seen that separation of the variables has increased the number of unknowns to seven, including $\bar{u}$, $\bar{v}$, $\bar{h}$, $\bar{p}_1$, $\bar{p}_2$, $\bar{\rho}$, $\bar{\mu}$. Similarly, the number of governing equations is now also seven, while the overall order of the mathematical system is eight requiring eight boundary conditions.

The boundary conditions become:

At $\bar{y} = 0$:

$$\bar{u}_w = 0, \quad \bar{v}_w = \bar{v}_w, \quad \bar{h}_w = \bar{h}_w \tag{44}$$

At $\bar{y} = \bar{\delta}_s$:

$$\bar{u}_s = 1, \quad \bar{v}_s = -1, \quad \bar{h}_s = (1-\epsilon^2), \quad \bar{p}_1 = (1-\epsilon), \quad \bar{p}_2 = 0 \tag{45}$$

The constraint equation becomes:

$$(1 + \bar{\delta}_s)^{1+j} + \bar{\rho}_w \bar{v}_w = \int_0^{\bar{\delta}_s} \frac{\bar{\rho}\bar{u}}{\epsilon} \left[2\,(1 + \bar{y}) \right]^j \, d\bar{y} \tag{46}$$

Here it is noted that for the special case of zero mass transfer, i.e. $\bar{\rho}_w \bar{v}_w = 0$, examination of eq. (37) indicates that the constraint

$$\bar{v}'_w = 0 \tag{47}$$

becomes identical with eq. (46). This latter result follows from the fact that since $\bar{u}_w$ and $\bar{v}_w$ are both zero (for zero mass transfer), unless $\bar{v}'_w$ also vanishes, one obtains the physically untenable result of an infinite density gradient at the wall, (Ref. 17).

In general, the transport properties depend on both temperature and composition. However, since the diffusion equations have been uncoupled, the composition of the gas is not calculated explicitly, and so it is necessary to resort to further approximations. Constant Prandtl and Lewis numbers have already been introduced and hence the thermal conductivity and the diffusion coefficients are not required explicitly. Thus, it remains to evaluate only the viscosity coefficient.

It is assumed that the gas is in chemical equilibrium, or more explicitly that the state of the gas can be determined from a Mollier diagram (e.g. Ref. 24). That is, knowledge of two state functions (e.g. pressure and enthalpy) uniquely determines the others (e.g. temperature, composition, density, etc.). It is assumed here that the viscosity coefficient can be approximated by Sutherland's formula for air (Ref. 25)

$$\mu = \mu\,(T) = 1.16 \times 10^{-5} \left(\frac{717}{225+T}\right)\left(\frac{T}{492}\right)^{3/2} \tag{48}$$

with T in $^{\circ}R$, μ is given in lb./ft.sec. However, since (from the Mollier diagram)

$$T = T\,(h,\ p) \tag{49}$$

then implicitly

$$\mu = \mu\,(h,\ p) \tag{50}$$

and the equation of state may also be obtained from the Mollier diagram i.e.

$$\rho = \rho\,(h,\ p) \tag{51}$$

Conditions behind the shock were determined from shock tables which incorporate the 1959 ARDC atmosphere, (Ref. 26).

Solutions were obtained on a Pace Electronics Associates high-speed electronic analog computer in the hypersonic low Reynolds number flight regime. Calculations were carried out for a range of flight speeds from 15,000 ft./sec. to 25,000 ft./sec., an altitude range from 175,000 ft. to 350,000 ft. for Reynolds numbers which were varied between 25 and 10^3, and a mass transfer parameter, $-0.4 \leq f_w \leq 0$. These results were compared with earlier theoretical studies in the continuum regime and in the low Reynolds number viscous layer regime (for zero mass transfer).

DISCUSSION OF RESULTS

The non-dimensional system of equations, (37) to (43), was solved on a Pace Electronics Associates analog computer. The equations were integrated from the wall out to the shock wave. Since the boundary conditions are split it is necessary to employ an iterative procedure. Some typical solutions for the viscous shock layer profiles of $\bar{u}$, $\bar{v}$, $\bar{h}$ and $\bar{p}$ are shown in Figures 3 to 6. As indicated by previous studies the viscous effects extend further into the shock layer with decreasing Reynolds number.

After numerous calculations for a wide range of altitudes, flight speeds, Reynolds numbers and wall temperatures, it was found that all of the data could be correlated with several standard non-dimensional ratios as functions of the Reynolds number alone. No discernible trends due to the other effects were noted.

Introducing the Stanton number

$$C_H = \frac{Q_w}{\rho_\infty V_\infty (H_s - h_w)} \tag{52}$$

all of the heat transfer data for zero mass transfer were correlated as a function of Reynolds number, and are shown in figure 7. Included in this figure are also some recent results of other investigators, Refs. 14, 17, 18, 27 and 28 for comparison. Here, it is seen that the present analysis indicates a larger low Reynolds number effect than predicted by the earlier investigators. In order to determine if these effects were due to the low Reynolds number nature of the flow, i.e. inclusion of all terms up to order $(Re_s)^{-1}$, or to the gas model chosen, new solutions were obtained for both Ho and Probstein's (Ref. 17), and Ferri, Zakkay and Ting's (Ref. 27)

analyses, utilizing the present gas model. These results which are based on the use of their differential equations, but our gas model, are shown in Figure 7 as curves 4 and 5. From these calculations, it is seen that the primary difference appears to be the gas model, since their original results shown as curves 2 and 3 of Figure 7 are shifted upwards and agree very well with the authors' results. It is also noted that for Reynolds numbers less than 10^3, the modified results, (curves 4 and 5) do not increase with decreasing Reynolds number as rapidly as the present computations. This result indicates the need to retain more higher-order terms with decreasing Reynolds number.

It may be noted that in checking the present system of equations, including the present gas model, at high Reynolds number ($Re_s = 2.5 \times 10^5$), the heat transfer was found to be approximately one percent different from more exact digital calculations based on using the high Reynolds number boundary layer equations and variable fluid properties, (Ref. 29).

The calculations in this study were carried out to Reynolds numbers below the range in which it is expected that the viscous flow layer will merge with the shock wave, in order to determine trends. From Refs. 17 and 27, it appears that the lower limit of the viscous layer regime is approximately $Re_s = 100$. Ho and Probstein (Ref. 17) extended their viscous layer results into the merged viscous layer regime by modifying a previous study (Ref. 14), (constant density solution). In a more recent study by Levinsky and Yoshihara (Ref. 18), the same system of equations and gas model employed by Probstein was solved from the free stream through the merged shock and viscous layer to the wall. The results are naturally similar, except that paradoxically they are shifted by an order of magnitude

to higher Reynolds numbers (See Figure 7), with some interesting consequences. At the higher Reynolds numbers the curve almost coincides with the authors' present results. Below a Reynolds number of about 10^3 the trend is downward indicating merged flow. An extension of the curve would appear to merge with results from a very recent experimental study by Dewey, Ref. 28. Dewey's tests were conducted at a nominal Mach number of 5.8 and stagnation temperature of 226°F explicitly ignoring dissociation.

It would appear from the divergence of the various theories and experimental data, that the low Reynolds number regime $Re_s < 10^2$ is not yet entirely understood.

With regard to skin friction, one observes that the surface shear stress is given by:

$$\tau_w = \left(\mu \frac{\partial u}{\partial y} \right)_w \tag{53}$$

and the skin friction coefficient by:

$$\tau_w = \frac{C_f}{2} \rho_\infty V_\infty^2 \tag{54}$$

The results of the computations of all skin friction data for zero mass transfer are shown in Figure 8. It is seen in this figure, as in the preceding one, that the present study shows a larger low Reynolds number effect than earlier studies.

Here it is seen that the dissociated gas model employed by the authors acts to increase the skin friction coefficient predicted by Refs. 17 and 27, (see curves 3 and 4 of Figure 8). However, at the lowest applicable Reynolds numbers the modified calculations remain twenty percent below the authors' results. This is actually not

surprising since most of the terms of order $(Re_s)^{-1}$ neglected in these earlier studies appear in the equation for the x-component of momentum, which is most influential in the determination of the shear stress.

In the presence of mass transfer, the energy transfer to the wall is given by (Ref. 29):

$$Q_w = (Q_w)_{\dot{m}_w = 0} + \left(\frac{\Delta\tilde{Q}}{\Delta\dot{m}}\right)_w \dot{m}_w \tag{55}$$

where the Q_w's and $(\Delta\tilde{Q}/\Delta\dot{m})_w$ have opposite signs and $\dot{m}_w = \rho_w v_w$. In the high Reynolds number regime at large flight speeds Scala has shown that $(\Delta\tilde{Q}/\Delta\dot{m})_w$ for air injection could be correlated, independent of pressure and geometry, by

$$\left(\frac{\Delta\tilde{Q}}{\Delta\dot{m}}\right)_w \approx 0.5\ (H_s - h_w) \tag{56}$$

when this "effectiveness quotient" is defined at $f_w = -0.4$ (large value of the mass transfer parameter). Figure 9 indicates that the high Reynolds number approximation is quite good down to Reynolds numbers as low as 10^3, for the prediction of $(\Delta\tilde{Q}/\Delta\dot{m})_w$.

For Reynolds numbers less than 10^3, the efficiency of the mass transfer process increases with decreasing Reynolds numbers. Note that the dimensionless mass transfer rate f_w is defined as:

$$-f_w = \frac{\rho_w v_w}{\sqrt{(1+j)\,\rho_w \mu_w \frac{du_s}{dx}}} \tag{57}$$

The reduction in skin friction with mass transfer is similarly given by (Ref. 5).

$$\tau = (\tau)_{\dot{m}_w = 0} - \left(\frac{\Delta \tau}{\Delta \dot{m}} \right)_w \dot{m} \qquad (58)$$

In Figure 10 the variation of $(\Delta \tau / \Delta \dot{m})_w$ with Reynolds number is shown. It was found that the new results are in agreement with Ref. 5 above $Re_s > 4 \times 10^4$. Here again, as in Figure 9, the effectiveness of the mass transfer process increases with decreasing Reynolds number.

In the high Reynolds number regime, the shock detachment distance is a function of body shape, density and velocity, independent of surface temperature and (moderate) mass transfer. However, at $Re_s < 4 \times 10^3$, the shock detachment distance is a function of body shape, flight speed, altitude, Reynolds number, wall temperature and mass transfer. This effect was investigated in order to predict the effects of mass transfer in the low Reynolds number viscous layer regime upon shock wave detachment distance. Figure 11 shows the variation of δ_s / R_B with the above parameters at a single altitude and flight speed. Intuitively, one expects that due to the extended interaction region, mass injection will push the shock further away from the body with decreasing Reynolds numbers. As seen in Figure 11, this is indeed found to be the case.

The asymptotic value of δ_s / R_B, in the high Reynolds number regime, was obtained from the theory developed by Li and Geiger, (Ref. 22).

CONCLUSIONS

1. Calculations based upon a dissociating perfect gas model predict that the heat transfer and skin friction will increase faster with decreasing Reynolds number, (for Reynolds numbers less than 10^4) than predicted by earlier theoretical studies using a non-dissociating perfect gas model.

2. Retention of all the higher order terms, up to terms of order $(Re_s)^{-1}$ indicates a slightly higher heat transfer rate at the lowest applicable Reynolds numbers, but a more significant increase in skin friction.

3. The benefits obtained with mass transfer in the high Reynolds number regime (reduction of skin friction and heat transfer) have been shown here to extend into the low Reynolds number regime. In fact, the two effectiveness quotients, $(\Delta\tilde{Q}/\Delta\dot{m})_w$ and $(\Delta\tau/\Delta\dot{m})_w$, which are indicative of the efficiency of the mass transfer process, increase with decreasing Reynolds number.

ACKNOWLEDGEMENT

The authors would like to acknowledge the assistance of Messers James D. Wigmore and Henry Bing of the Simulation Technology group and Nicholas Macri and Charles Cook of the High Altitude Aerodynamics Operation for assisting in the computations and in the preparation of the graphs. The analysis is based on work performed under the auspices of the U.S. Air Force, B.S.D. contract no. AF 04-(647)-617.

REFERENCES

1. Hayes, W. D. and Probstein, R. F., "Hypersonic Flow Theory", Academic Press, New York, 1959.

2. Lees, T., "Laminar Heat Transfer Over Blunt Bodies at Hypersonic Flight Speeds", Jet Propulsion, Vol. 26, pp 259-269, 1956.

3. Fay, J. A. and Riddell, F. R., "Theory of Stagnation Point Heat Transfer in Dissociated Air", J. Aero. Sci., Vol. 25, pp. 78-85, 1958.

4. Scala, S. M., "A Study of Hypersonic Ablation", Proceedings of the Tenth International Astronautical Federation Congress, London, Springer Verlag, pp. 790-828, 1959.

5. Scala, S. M. and Ashley, W. F., "Mass Addition Effects on Hypersonic Heat Transfer to a Two-Dimensional Body", Proceedings of the 1961 International Heat Transfer Conference, Univ. of Colorado, Boulder, Colorado, pp. 696-706, 1961.

6. Gilbert, L. M. and Scala, S. M., "Free Molecular Heat Transfer in the Ionosphere", AAS Preprint 61-72, to appear in the Proceedings of the American Astronautical Society Symposium on Interactions of Space Vehicles with an Ionized Atmosphere, Washington, D. C., 1961.

7. Wachman, H. Y., "The Effect of Surface Properties on Energy Transfer at Low Gas Densities", Proceedings of General Electric Co. MSVD, High Altitude Aerodynamics Conference, Paper 2.3, 1961.

8. Wachman, H. Y., "The Thermal Accomodation Coefficient: A Critical Survey", A.R.S. Journal, Vol. 32, No. 1, p. 1, 1962.

9. Hartnett, J. P., "A Survey of Thermal Accomodation Coefficients", Proceedings of the Second Rarefied Gas Dynamics Symposium, Academic Press, pp. 1-28, 1960.

10. Willis, D. R. "A Study of Some Nearly Free Molecular Flow Problems", Ph. D. dissertation, Princeton University, Princeton, New Jersey, 1958.

11. Baker, R. M. L. Jr. and Charwat, A. F., "Transitional Correction to the Drag of a Sphere in Free Molecule Flow", Phys. Fluids, Vol. 1, pp. 73-81, 1958.

12. Enoch, J., "A Kinetic Model for Hypersonic Rarefied Gas Flow", General Electric Co., MSVD TIS R61SD063, 1961.

13. Hoshizaki, H., "Shock-Generated Vorticity Effects at Low Reynolds Numbers", Lockheed Missiles and Space Division, LMSD 48381, Vol. I, pp. 9-43, Jan. 1959.

14. Probstein, R. F. and Kemp, N. H., "Viscous Aerodynamic Characteristics in Hypersonic Rarefied Gas Flow", J. Aero. Sci., Vol. 27, pp. 174-192, 218, 1960.

15. Oguchi, H., "Blunt Body Viscous Layer With and Without a Magnetic Field", Phys. of Fluids, Vol. 3, pp. 567-580, 1960.

16. Hoshizaki, H., Neice, S. and Chan, K. K., "Stagnation Point Heat Transfer Rates at Low Reynolds Numbers", IAS Preprint 60-68, Presented at IAS Nat. Sum. Meet., June 28 - July 1, 1960.

17. Ho, H. T. and Probstein, R. F., "The Compressible Viscous Layer in Rarefied Hypersonic Flow", Brown University, ARL TN 60-132, Aug. 1960. Also published in Proceedings of the Second Rarefield Gas Dynamics Symposium, Academic Press pp. 525-552, 1960.

18. Levinsky, E. S. and Yoshihara, H., "Rarefied Hypersonic Flow Over a Sphere", Presented at the ARS International Hypersonics Conference, MIT, Cambridge, Massachusetts, 1961.

19. Talbot, L. and Scala, S. M., "Shock Wave Structure in a Relaxing Diatomic Gas", Proceedings of the Second International Symposium on Rarefied Gas Dynamics, Berkeley, California, pp. 603-622, 1960.

20. Chung, P. M., "Hypersonic Viscous Shock Layer of Non-equilibrium Dissociating Gas", NASA TR R-109, 1961.

21. Chapman, S. and Cowling, T.G., "The Mathematical Theory of Non-Uniform Gases", University Press, Cambridge, 1958.

22. Li, T.Y. and Geiger, R.E., "Stagnation Point of a Blunt Body in Hypersonic Flow", J. Aero. Sci., Vol. 24, pp. 25-32, 1957.

23. Hirshfelder, J.O. and Curtiss, C.F. and Bird, R.B., "Molecular Theory of Gases and Liquids", John Wiley and Sons, Inc., 1954.

24. Moeckel, W.E. and Weston, K.C., "Composition and Thermodynamic Properties of Air in Chemical Equilibrium", NACA TN 4265, 1958.

25. Jeans, J.H., "The Dynamical Theory of Gases", Dover Publications, Inc., New York, 1954.

26. Cook, C., Gilbert, L. and Scala, S.M., "Normal Shock and Stagnation Point Solutions for Equilibrium Dissociated Air", to be published.

27. Ferri, A., Zakkay, V. and Ting, L., "Blunt Body Heat Transfer at Hypersonic Speed and Low Reynolds Numbers", J. Aero. Sci., Vol. 28, pp. 962-971, 991, 1961.

28. Dewey, C.F., Jr., "Hot Wire Measurements in Low Reynolds Number Hypersonic Flows", ARS Journal, Vol. 31, pp. 1709-1718, 1961.

29. Scala, S.M., "Transpiration Cooling in the Hypersonic Laminar Boundary Layer", General Electric Co. MSVD TIS 58SD215, March, 1958.

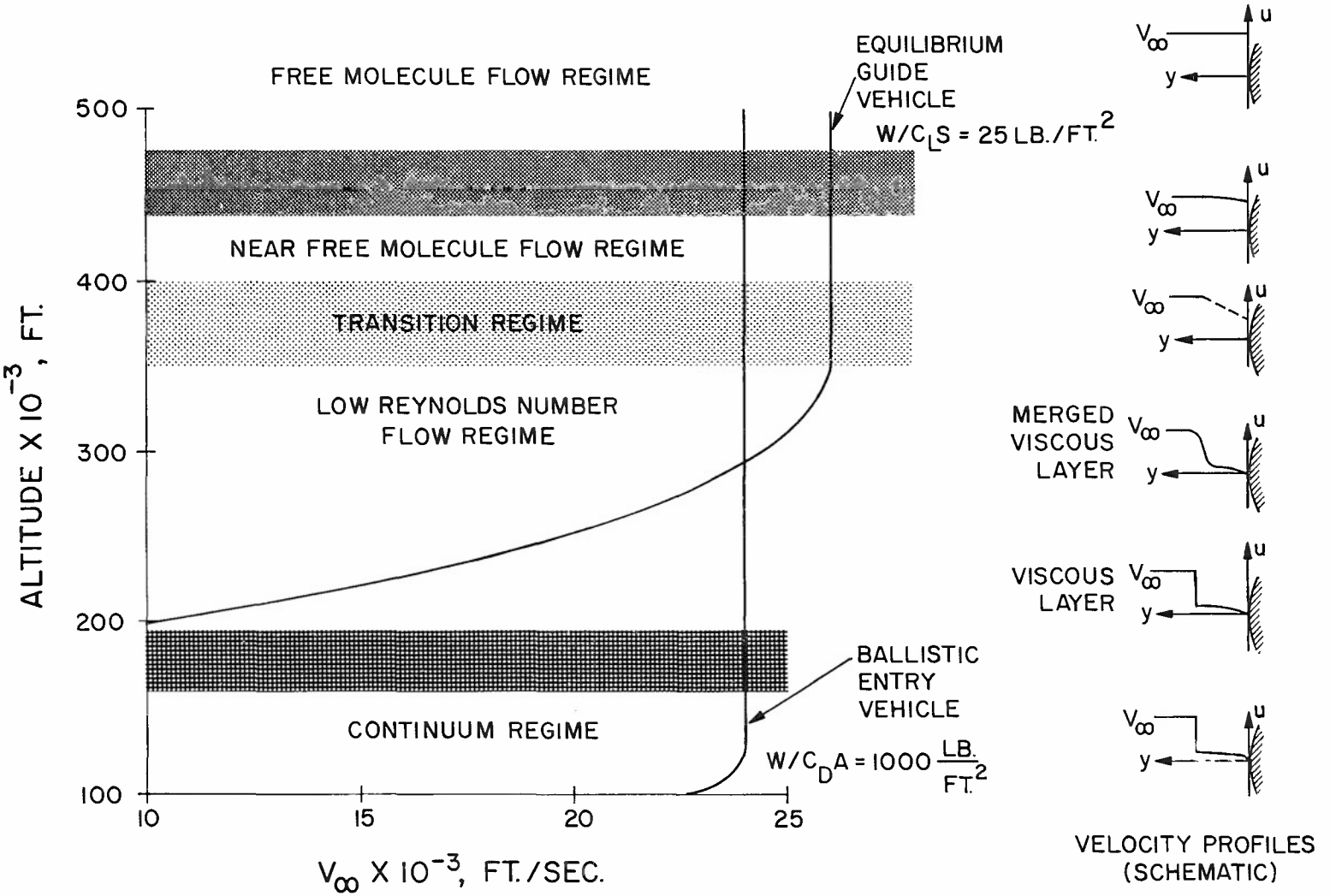
HIGH ALTITUDE HYPERSONIC FLIGHT REGIMES, $R_B \approx 0.1$ FT.
FREE MOLECULE FLOW REGIME
NEAR FREE MOLECULE FLOW REGIME
TRANSITION REGIME
LOW REYNOLDS NUMBER FLOW REGIME
CONTINUUM REGIME
EQUILIBRIUM GUIDE VEHICLE
$W/C_L S = 25$ LB./FT.^{2}
BALLISTIC ENTRY VEHICLE
$W/C_D A = 1000 \frac{LB.}{FT.^2}$
ALTITUDE X 10^{-3}, FT.
500
400
300
200
100
10
15
20
25
V_∞ X 10^{-3}, FT./SEC.
MERGED VISCOUS LAYER
VISCOUS LAYER
V_∞
y
u
VELOCITY PROFILES (SCHEMATIC)

FIG. 1

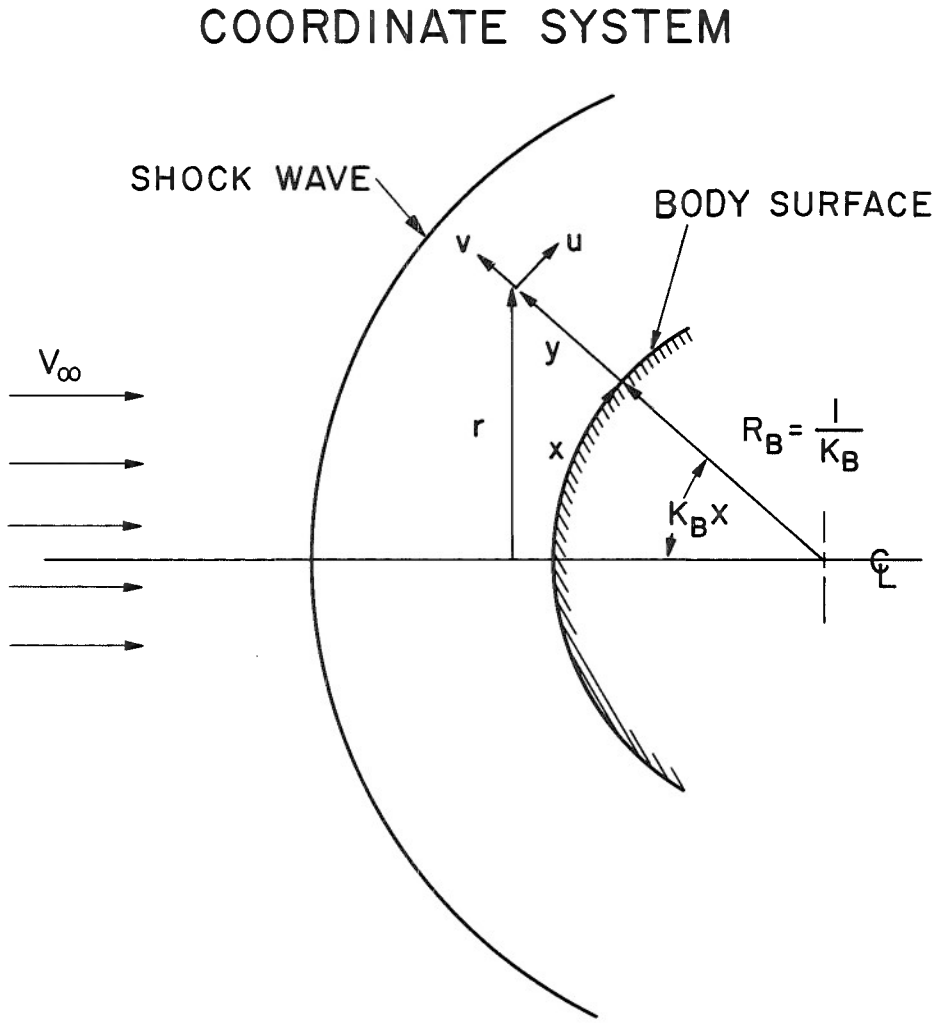
COORDINATE SYSTEM
SHOCK WAVE
BODY SURFACE
v
u
y
r
x
V_∞
$R_B = \frac{1}{K_B}$
$K_B x$
C_L

FIG. 2

VISCOUS LAYER PROFILES IN THE STAGNATION REGION OF A SPHERE, $RE_S = 10^3$

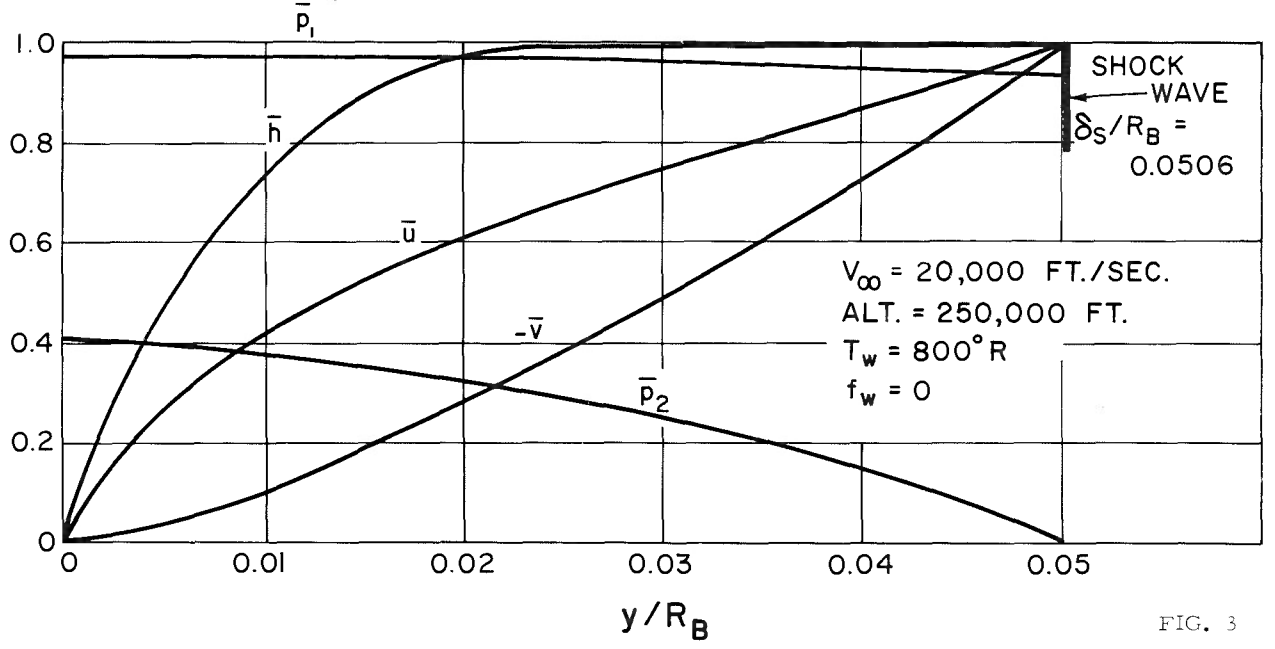

FIG. 3

VISCOUS LAYER PROFILES IN THE STAGNATION REGION OF A SPHERE, $RE_S = 10^2$

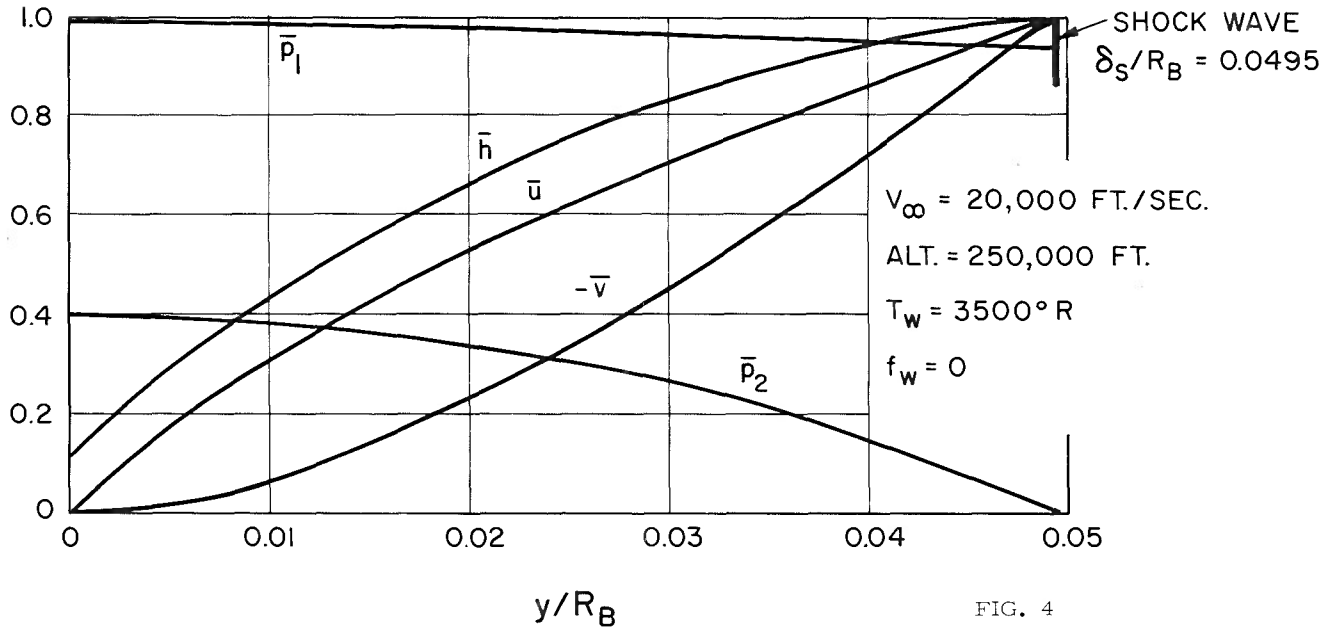

FIG. 4

VISCOUS LAYER PROFILES IN THE STAGNATION REGION OF A SPHERE, $Re_S = 25$

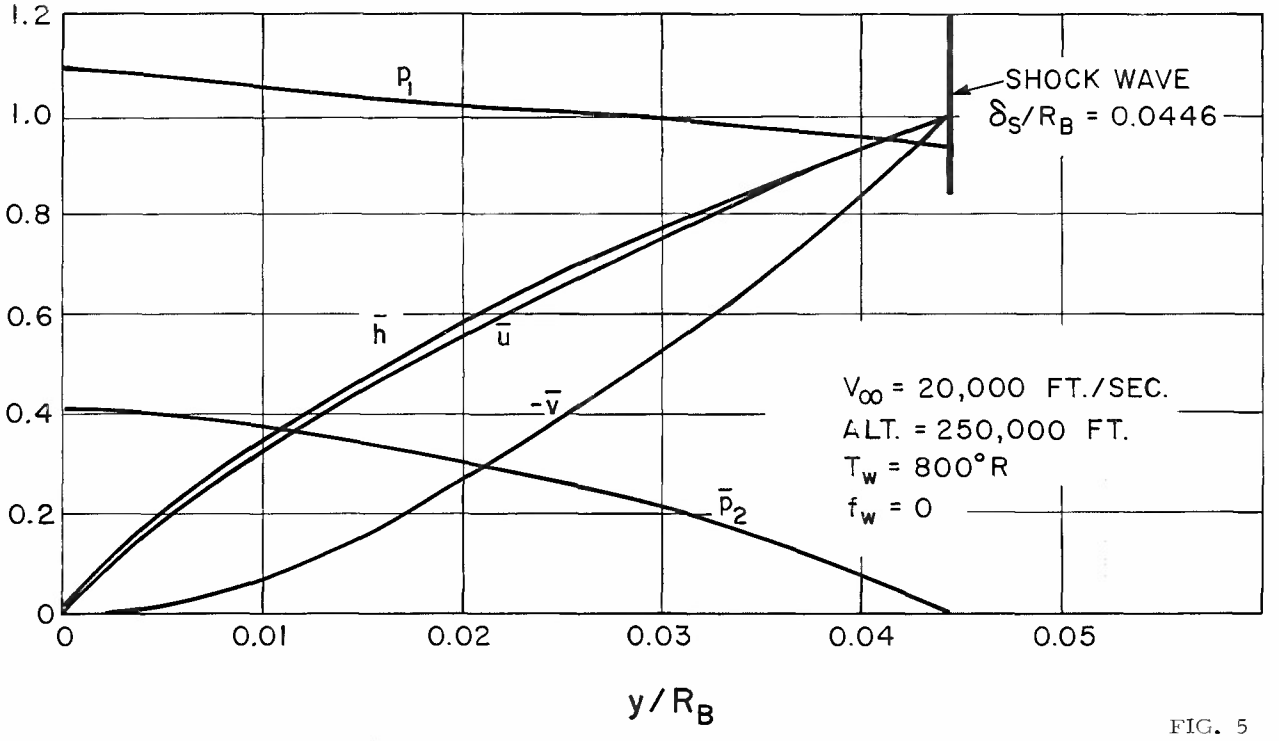

FIG. 5

VISCOUS LAYER PROFILES IN THE STAGNATION REGION OF A SPHERE, $RE_S = 25$

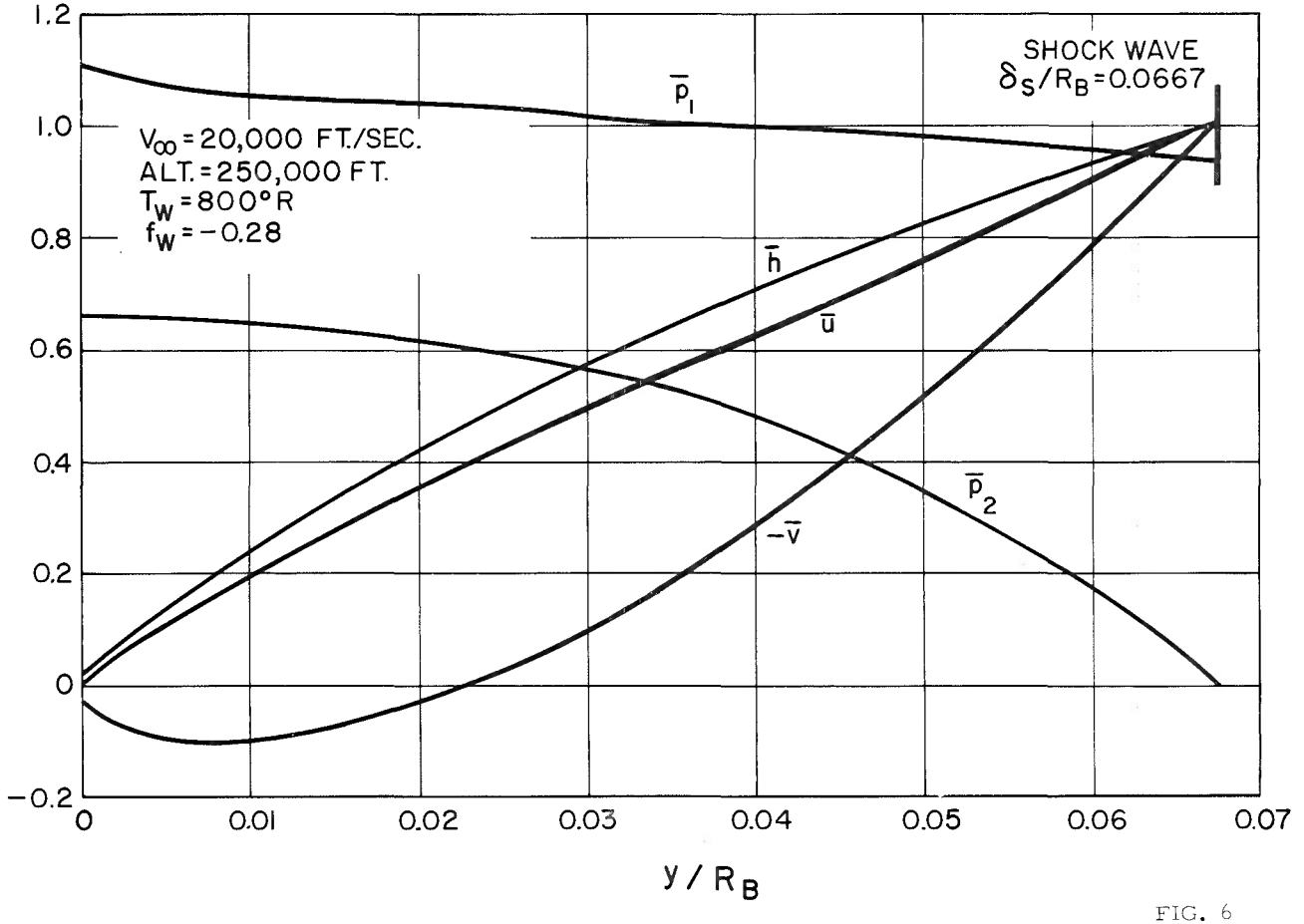

FIG. 6

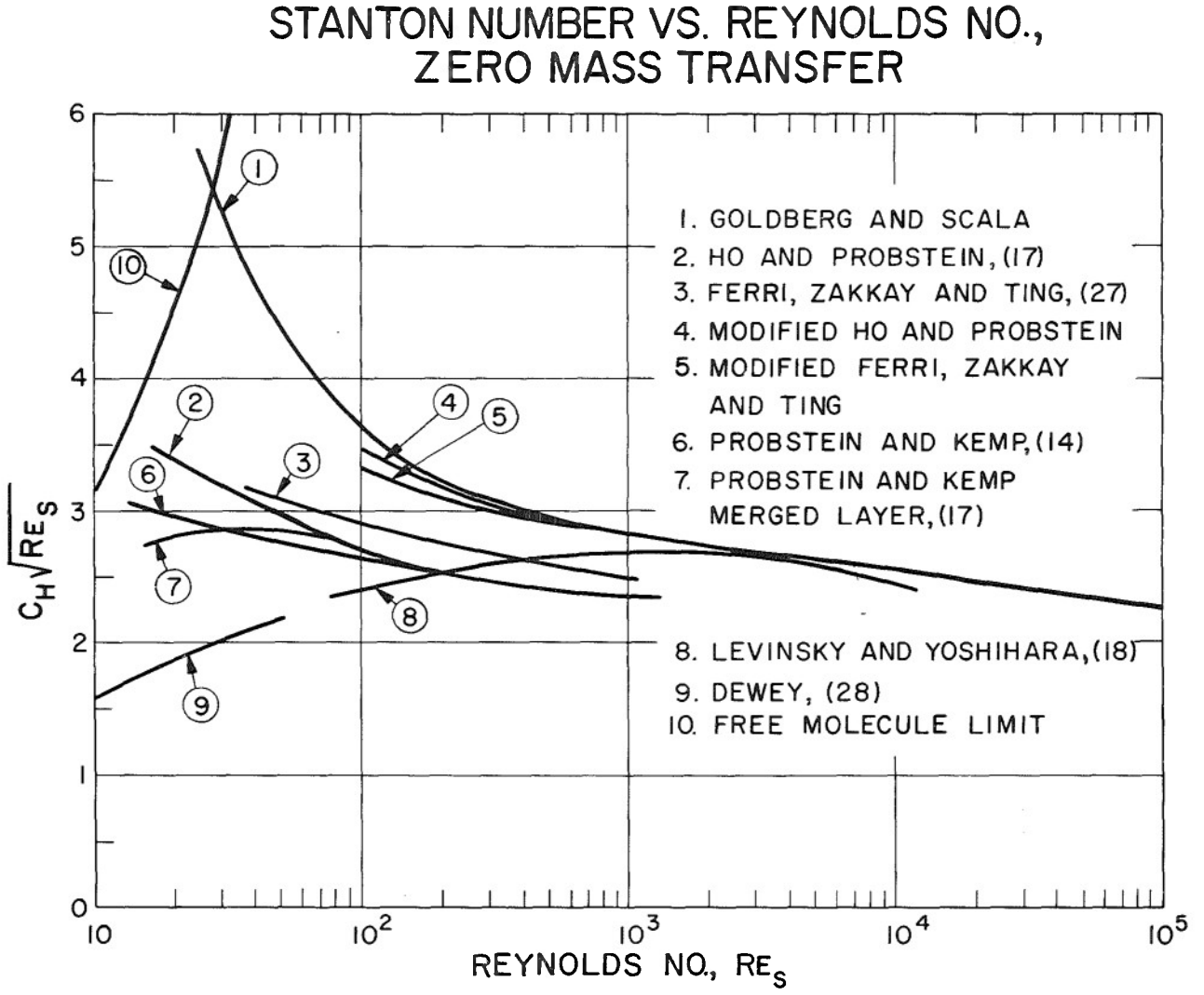
STANTON NUMBER VS. REYNOLDS NO.,
ZERO MASS TRANSFER
1. GOLDBERG AND SCALA
2. HO AND PROBSTEIN, (17)
3. FERRI, ZAKKAY AND TING, (27)
4. MODIFIED HO AND PROBSTEIN
5. MODIFIED FERRI, ZAKKAY AND TING
6. PROBSTEIN AND KEMP, (14)
7. PROBSTEIN AND KEMP MERGED LAYER, (17)
8. LEVINSKY AND YOSHIHARA, (18)
9. DEWEY, (28)
10. FREE MOLECULE LIMIT
$C_H\sqrt{RE_S}$
REYNOLDS NO., RE_S
0
1
2
3
4
5
6
10
10^2
10^3
10^4
10^5

FIG. 7

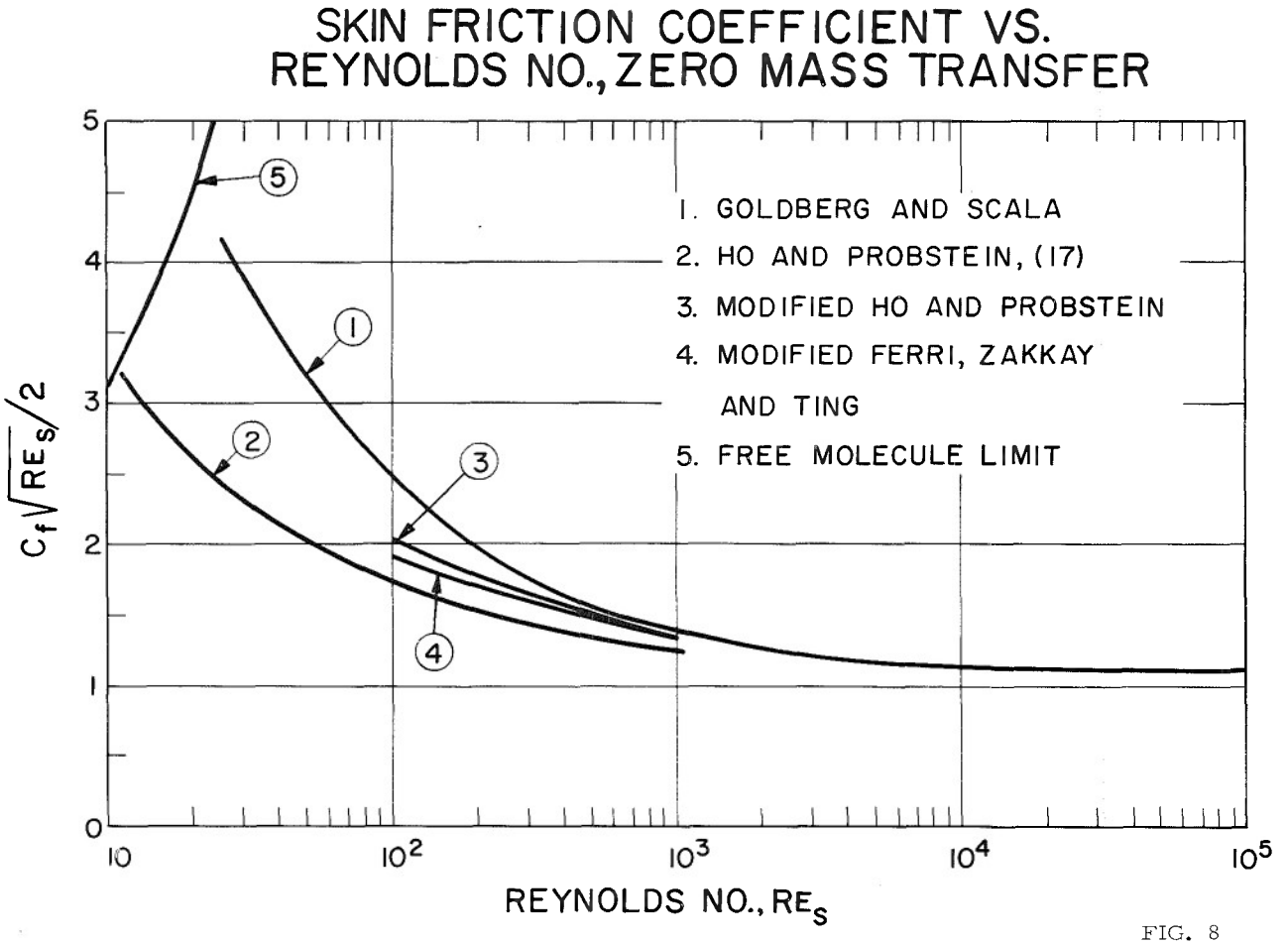
SKIN FRICTION COEFFICIENT VS.
REYNOLDS NO., ZERO MASS TRANSFER
1. GOLDBERG AND SCALA
2. HO AND PROBSTEIN, (17)
3. MODIFIED HO AND PROBSTEIN
4. MODIFIED FERRI, ZAKKAY AND TING
5. FREE MOLECULE LIMIT
$C_f\sqrt{RE_s}/2$
REYNOLDS NO., RE_s
0
1
2
3
4
5
10
10^2
10^3
10^4
10^5

FIG. 8

REDUCTION IN ENERGY TRANSFER WITH MASS TRANSFER VS. REYNOLDS NO.

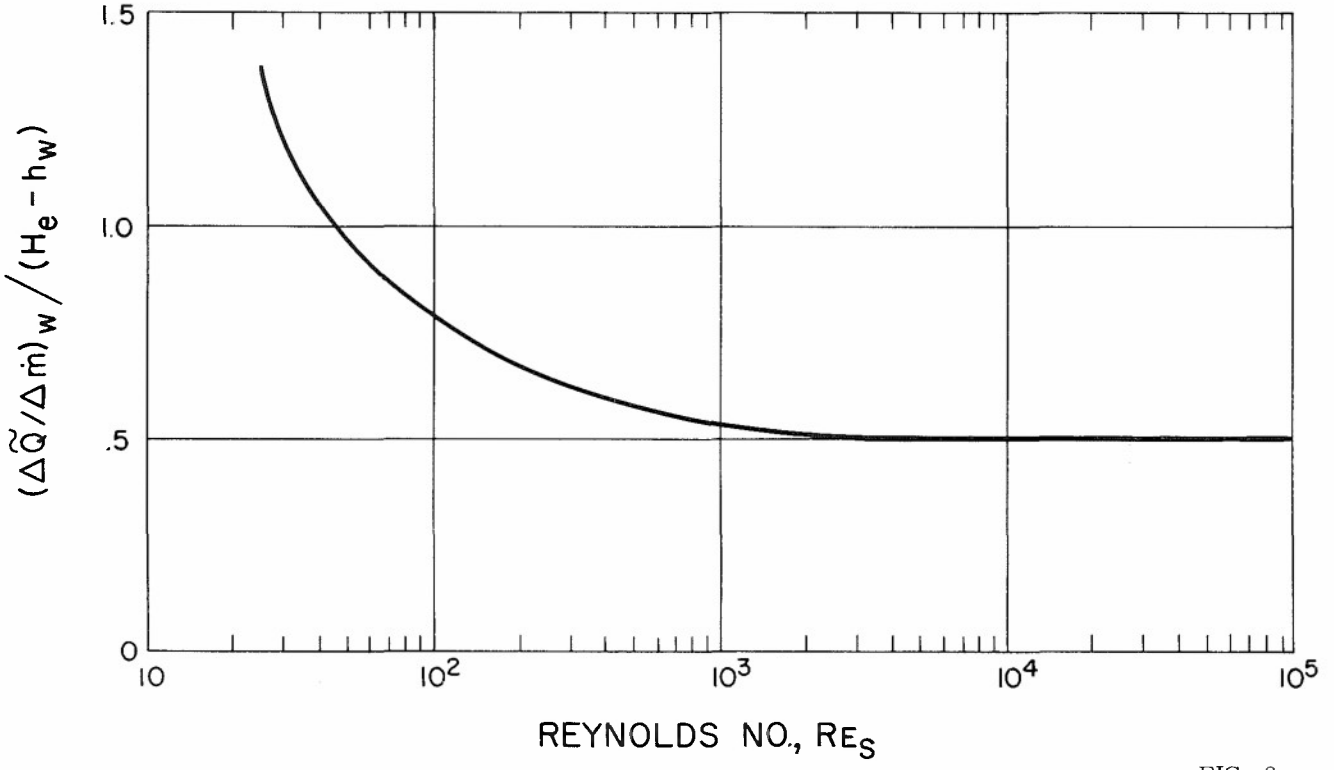

FIG. 9

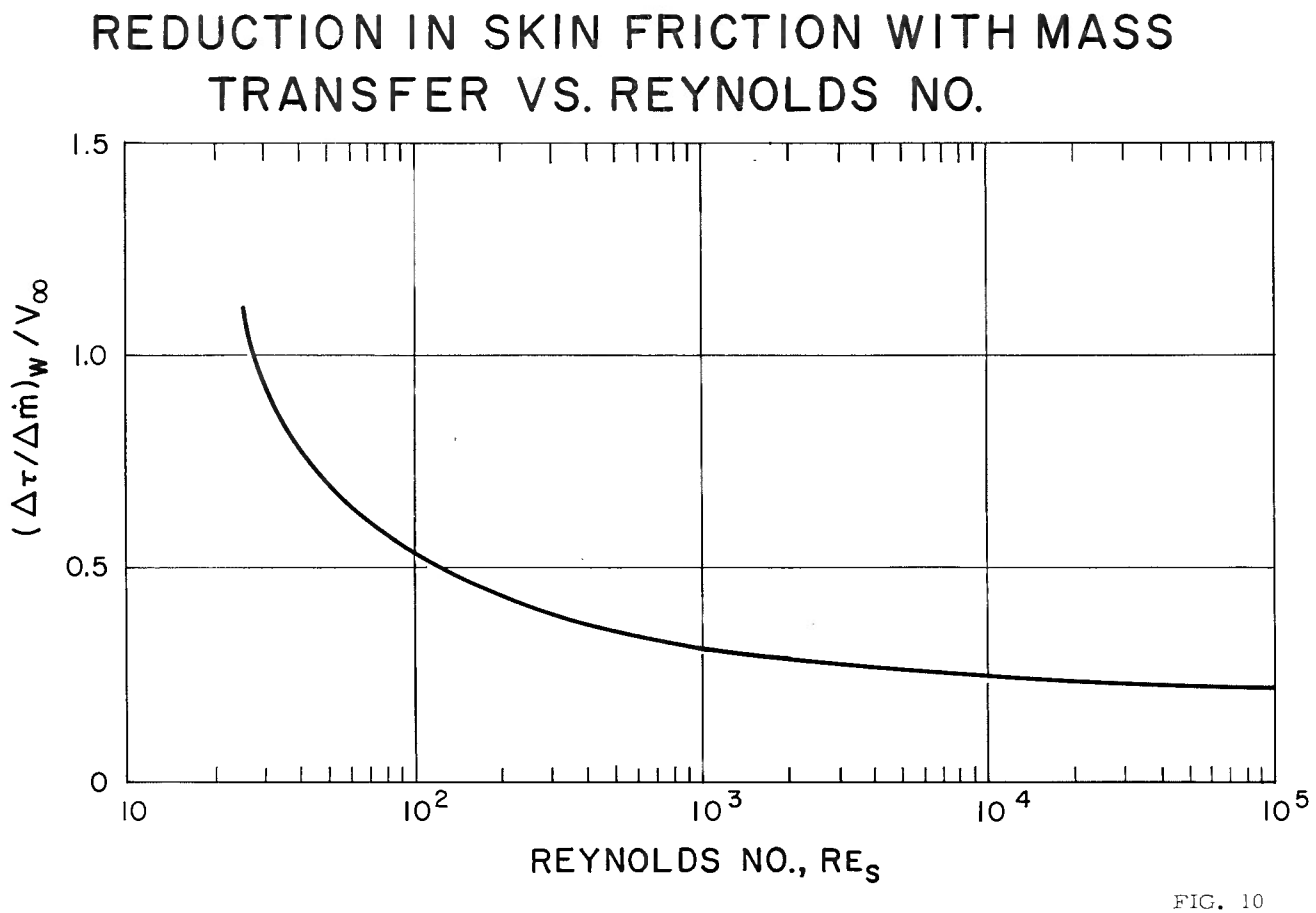
REDUCTION IN SKIN FRICTION WITH MASS TRANSFER VS. REYNOLDS NO.
1.5
1.0
0.5
0
$(\Delta\tau/\Delta\dot{m})_w/V_\infty$
10
10^2
10^3
10^4
10^5
REYNOLDS NO., RE_s

FIG. 10

SHOCK DETACHMENT DISTANCE VERSUS REYNOLDS NO. AND DIMENSIONLESS MASS TRANSFER RATE

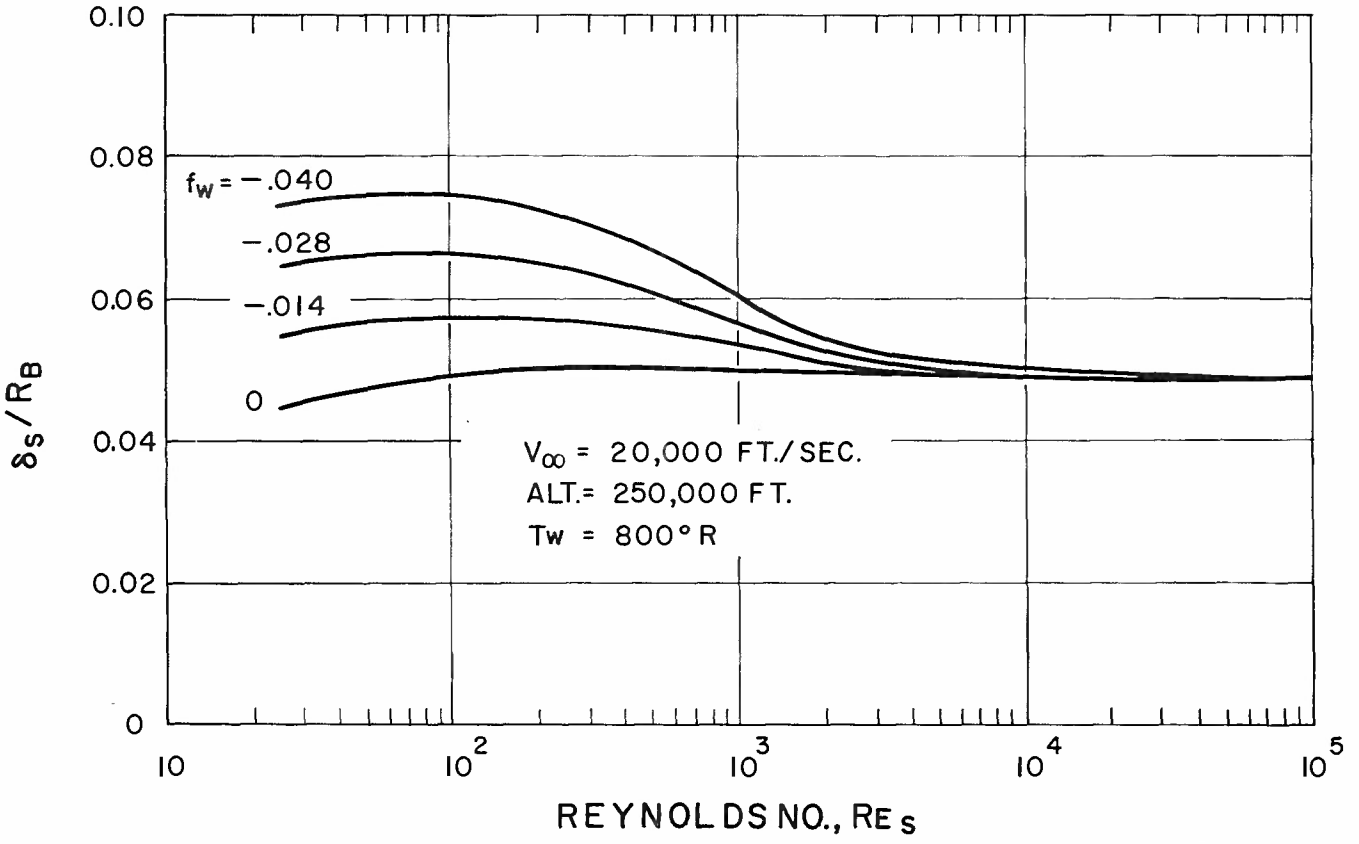

FIG. 11

GENERAL ELECTRIC

SPACE SCIENCES LABORATORY
MISSILE AND SPACE VEHICLE DEPARTMENT

TECHNICAL INFORMATION SERIES

AUTHOR	SUBJECT CLASSIFICATION	NO.
L. Goldberg S. M. Scala	Hypersonic Aerodynamics, Low Reynolds Number Effects, Mass Transfer	R62SD07
		DATE 1/15/62

TITLE

MASS TRANSFER IN THE HYPERSONIC LOW REYNOLDS NUMBER VISCOUS LAYER*

ABSTRACT

A study is presented of the low Reynolds number effects encountered by a re-entry vehicle traveling at hypersonic speeds in the Earth's atmosphere. Included are real gas effects such as dissociation, and mass transfer from the surface.

G. E. CLASS	REPRODUCIBLE COPY FILED AT	NO. PAGES
1	G. E. TECHNICAL INFORMATION CENTER 3198 CHESTNUT STREET PHILADELPHIA, PENNA.	42
GOV. CLASS Unclassified		

CONCLUSIONS

1. Calculations based upon a dissociating gas model predict larger heat transfer and skin friction in the low Reynolds number regime than predicted by earlier theoretical studies using a non-dissociating perfect gas model.

2. Retention of all the higher order terms, up to terms of order $(Re_s)^{-1}$ indicates a slightly higher heat transfer at the lowest applicable Reynolds numbers, but a more significant increase in skin friction.

3. The benefits of mass transfer (reduction in heat transfer and skin friction) have been shown here to extend into the low Reynolds number regime. In fact, the efficiency of the mass transfer process increases with decreasing Reynolds number.

*This paper was presented at the IAS 30th Annual Meeting, New York City, New York, January 22, 1962, Preprint No. 62-80.

By cutting out this rectangle and folding on the center line, the above information can be fitted into a standard card file.

AUTHOR L. Goldberg S. M. Scala

COUNTERSIGNED J. Farber

DIVISION Defense Electronics

LOCATION Valley Forge, Pennsylvania